INTERNATIONAL JOURNAL OF CLIMATOLOGY
Int. J. Climatol. **34**: 3986–3997 (2014)
Published online 8 April 2014 in Wiley Online Library
(wileyonlinelibrary.com) DOI: 10.1002/joc.3998

The impact of two land-surface schemes on the characteristics of summer precipitation over East Asia from the RegCM4 simulations

Suchul Kang,[a,b] Eun-Soon Im[c]* and Joong-Bae Ahn[b]
[a] *APEC Climate Center, Busan, Korea*
[b] *Division of Earth Environmental System, Pusan National University, South Korea*
[c] *Center for Environmental Sensing and Modeling, Singapore-MIT Alliance for Research and Technology, Singapore*

ABSTRACT: This study evaluates the performance of the regional climate model RegCM4, which incorporates the Biosphere–Atmosphere Transfer Scheme (BATS) and Community Land Model (CLM3) land-surface schemes, in simulating the summer precipitation over East Asia. The characteristics of summer precipitation are analysed in terms of mean amount, frequency and intensity of daily precipitation. The results show that the simulation of the summer precipitation is significantly sensitive to the choices of the land-surface schemes. Despite several deficiencies, the simulation of daily precipitation with CLM3 exhibits superior performance to that with BATS. The BATS simulation tends to systematically overestimate both precipitation frequency and intensity, and hence total precipitation across the whole domain. On the other hand, the CLM3 simulation substantially reduces the wet biases produced in the BATS simulation. The difference in performance between the two simulations mainly results from convective precipitation rather than large-scale precipitation. Since excessive convective precipitation tends to suppress large-scale precipitation, the BATS simulation also exhibits a limitation in properly simulating the ratio of convective and large-scale precipitation. Such behaviour can be explained by the influence of soil moisture on convective precipitation. Persistently wetter soil moisture in the BATS land-surface scheme can modulate the partitioning of surface heat fluxes inadequately, leading to overestimation of latent heat flux and underestimation of sensible heat flux over South China, in particular. Consequently, it affects the thermodynamic structure (as described by the stability indices), which in turn affects the atmospheric stability to determine the convective activity. The CLM3 simulation generates a more realistic representation of equivalent potential temperature, convective available potential energy and convective inhibition, and thus improves the characteristics of daily precipitation.

KEY WORDS RegCM4; land-surface scheme; summer precipitation

Received 8 October 2013; Revised 30 January 2014; Accepted 3 March 2014

1. Introduction

Over the past decades, significant progress has been made in improving the performance in simulating summer precipitation over East Asia. In particular, various attempts have been conducted within the framework of regional climate models (RCMs) with relatively higher resolution than that of global climate models (e.g. Fu *et al.*, 2005; Kang *et al.*, 2005; Yhang and Hong, 2008; Park *et al.*, 2013). Since summer precipitation over East Asia is a product of a number of processes such as complicated multi-scale interactions among atmosphere, land and ocean, as well as local processes related to the complex and unique geographical setting of the Asian continent, a higher resolution model is useful for improving results in capturing the detailed characteristics of regional-scale climate (Gao *et al.*, 2008; Min and Jhun, 2010; Chen *et al.*, 2012).

Although RCMs are the ultimate tool for producing physically based fine-scale climate information, they suffer from the large sensitivity and uncertainty of physical parameterizations that directly affect the reliability of model performance (Cha *et al.*, 2008). The difficulty of incorporating or modifying physical schemes is the absence of any universally superior physical scheme because its performance varies according to the region, season and combination with other schemes. Therefore, it is important to use appropriate physical parameterizations for the selected target region in order to optimize the model performance. Over East Asia, many studies have attempted to improve the precipitation skill during the summer season based on the cumulus convection schemes (Hong and Choi, 2006; Singh *et al.*, 2006; Im *et al.*, 2008; Kang and Hong, 2008; Oh *et al.*, 2011; Huang *et al.*, 2012; Bao, 2013). Although the precipitation pattern is directly affected by the cumulus convection scheme and its interaction with other physical processes, the land-surface scheme can also be important in determining the performance of precipitation over East Asia. For example, Chen

* Correspondence to: Dr. Eun-Soon Im, Singapore-MIT Alliance for Research and Technology (SMART) Center for Environmental Sensing and Modeling (CENSAM), 1 CREATE Way, #09-03 CREATE Tower, Singapore 138602, Singapore. E-mail: eunsoon@smart.mit.edu

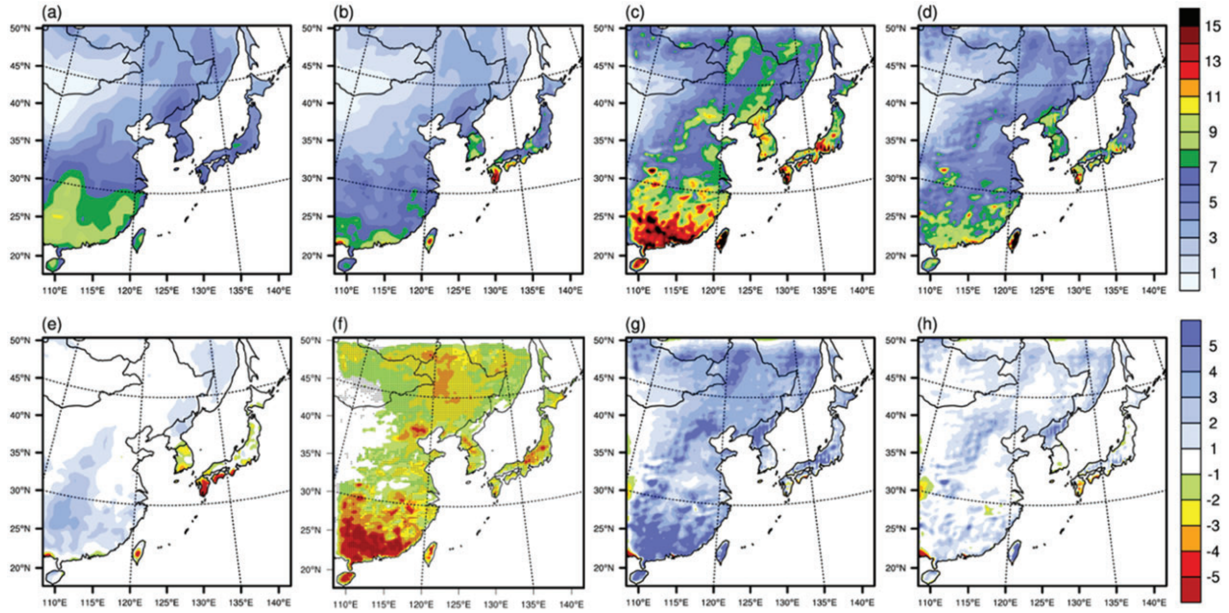

Figure 1. Spatial distribution of JJA mean precipitation derived from ERA–interim, APHRODITE, BATS and CLM3 simulations (a–d) and their differences between ERA–interim and APHRODITE (e), the two simulations CLM3–BATS (f), and the two simulations APHRODITE, BATS–APHRODITE (g) and CLM3–APHRODITE (h) (mm day^{-1}). Here, superimposed dots in (f) indicate the areas where the differences are statistically significant at the 99% confidence level.

et al. (2012) demonstrated that the Community Land Model (CLM3.5) can greatly improve precipitation and temperature in eastern China compared to the Community NOAH land-surface scheme when coupled to the Weather Research and Forecasting (WRF). Steiner *et al.* (2005) also showed the role of the land-surface scheme in modulating the surface energy and water budget by replacing the Biosphere–Atmosphere Transfer Scheme (BATS) with CLM0 in the RegCM. However, as both studies were based on a single-year simulation, it is difficult to derive a general and robust conclusion. In this regard, further investigation is necessary to determine the impact of the land-surface scheme in simulating the climate over East Asia.

The most significant difference in the latest version of the International Centre for Theoretical Physics (ICTP) RCM (e.g. RegCM4) relative to the previous versions of the model (e.g. RegCM3) is coupling with CLM3 (Giorgi *et al.*, 2012). In this study, we build on previous findings of the sensitivity of the East Asia summer monsoon to the land-surface scheme by comparing the high-resolution (30 km) multi-decadal (19 years) simulations that implement two different land-surface schemes (BATS *vs* CLM3) available in RegCM4, which is considered the state-of-the-art simulation in terms of resolution and period. Our focus is to investigate the impact of the land-surface scheme on the characteristics of summer precipitation from the perspective of the convective instability. Sensitivity studies have mostly been limited to evaluating and comparing the mean state of several climate variables (e.g. Chen *et al.*, 2012), and little focus has been paid to how the land-surface scheme affects triggering or strengthening of the convection in simulating the summer precipitation over East Asia. Such an investigation might improve our understanding of the control factor that determines the different characteristics of precipitation by different land-surface schemes. This study will contribute to a more accurate estimation of the relative strength and weakness of the RegCM4 modelling system incorporating the BATS and CLM3 land-surface schemes over East Asia.

2. Model and experimental design

2.1. RegCM4 description

The RCM used in this study is the latest version of the ICTP RCM RegCM4. RegCM4 is built on RegCM3 but with several improvements as described by Giorgi *et al.* (2012). The dynamical core is equivalent to the hydrostatic version of the NCAR/Pennsylvania State University Mesoscale Model Version 5 (MM5, Grell *et al.*, 1994). The physical parameterizations used in the default RegCM4 configuration include the comprehensive radiative transfer package of the NCAR Community Climate Model Version 3 (CCM3, Kiehl *et al.*, 1996), the non-local boundary layer scheme of Holtslag *et al.* (1990), and the Sub-grid Explicit Moisture Scheme (SUBEX) of Pal *et al.* (2000) for resolvable grid-scale precipitation. Among several options for convective parameterization, the MIT Emanuel scheme (Emanuel and Zivkovic-Rothman, 1999) is selected based on several previous studies that demonstrated its superiority over East Asia (Singh *et al.*, 2006; Im *et al.*, 2008; Oh *et al.*, 2011).

RegCM4 incorporates the multiple options of the land-surface schemes through the newly coupled CLM3, in addition to the original existing BATS scheme. CLM3, which was developed and supported by NCAR, is a ‘third-generation’ land-surface parameterization that

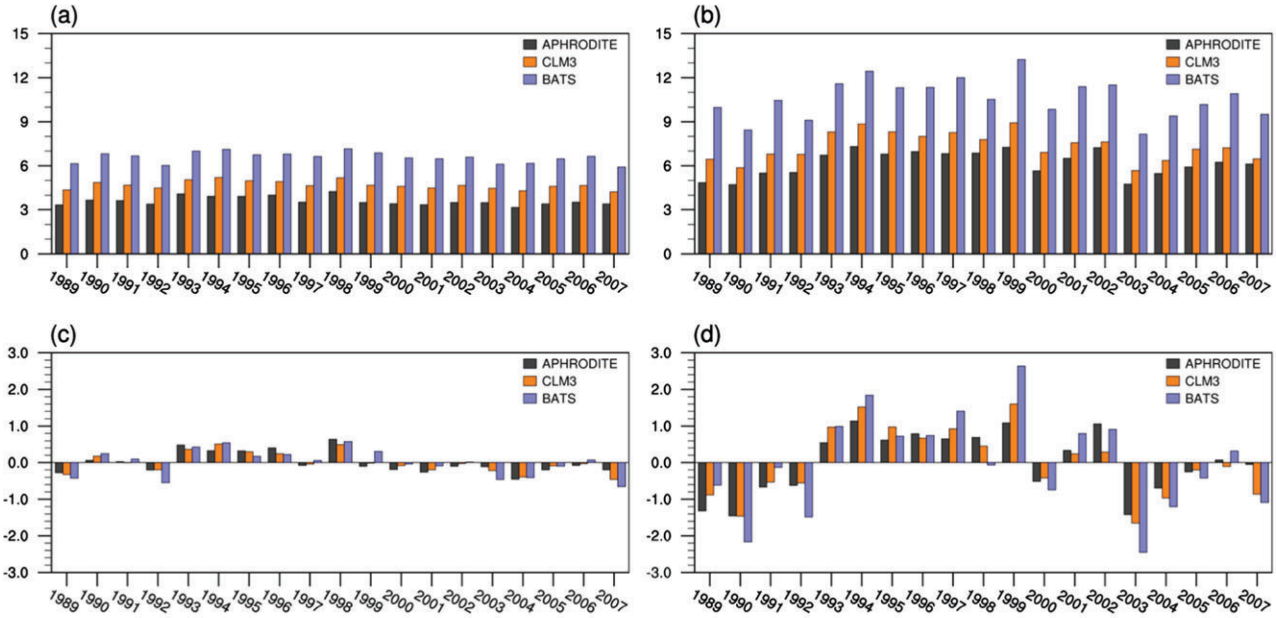

Figure 2. Interannual variability of JJA mean precipitation averaged over entire domain and South China and its anomaly with respect to mean climatology derived from APHRODITE, BATS and CLM3 simulations. (a,c) Entire domain, (b,d) South China.

includes the land–atmosphere exchanges of energy, momentum, water and carbon. CLM3 is considered a more complex and advanced model than BATS because of its finer vertical soil and snow layer resolution, tiling structure, subsurface lateral runoff and direct calculation of carbon. Further details of both BATS and CLM3 schemes are presented in Steiner *et al.* (2005, 2009).

2.2. Experimental design

The simulation domain covers the eastern regions of the huge Asia continent and the Japanese Archipelago with the centre on the Korean peninsula (see Figure 1; each panel shows the simulation domain excluding the buffer zone). The horizontal resolution is 30 km with 129 (North-South direction) × 129 (East-West direction) grid points, while 23 vertical levels are used within the sigma coordinator.

The initial and lateral boundary conditions are obtained from the ERA–interim reanalysis with a resolution of 1.5° × 1.5° at 6-hour intervals (Dee *et al.*, 2011). The simulations start from 25 May and span 7 days and three months (June–July–August: JJA) in every year of the 19-year period (1989–2007), and the results during the first 7 days are excluded in the analysis as a spin-up period. To justify this spin-up period, we examined the sensitivity of the length of spin-up by comparing the experiments with different spin-up period (7 days *vs* 1 month) for the first 1 year (1989) during our simulation period. We found that the difference of JJA mean precipitation between the two simulations seems to be random and trivial (Figures S1 and S2). In fact, Anthes *et al.* (1989) demonstrated that regional models attain the dynamical equilibrium between the lateral forcing and the internal physical dynamics of the model in about 2–3 days. The two simulation sets are integrated by implementing the BATS and CLM3 land-surface schemes, with all other conditions being identical.

Both observation and reanalysis datasets are used to validate the performance of the simulations. To assess the performance of daily precipitation, we use daily precipitation with 0.25° × 0.25° grid provided by the Asian Precipitation Highly Resolved Observational Data Integration Towards the Evaluation of Water Resources project (APHRODITE, Yatagai *et al.*, 2009), as well as 1.5° × 1.5° grid from ERA–interim reanalysis (Dee *et al.*, 2011). The daily vertical dataset (e.g. temperature, dew point temperature and geopotential height) for the calculation of the convective available potential energy (CAPE) and convective inhibition (CIN) is also extracted from the ERA–interim reanalysis. The simulated latent and sensible heat fluxes are evaluated against the ERA–interim reanalysis on a monthly basis.

3. Results

We begin our analysis with the 19-year climatological aspects of precipitation during the summer season (JJA). The upper panels in Figure 1 present the spatial distribution of JJA mean precipitation derived from ERA–interim reanalysis, APHRODITE observation and BATS and CLM3 simulations. First, in spite of the general agreement, ERA–interim with a resolution of 1.5° × 1.5° shows rather different features with a finer resolution of APHRODITE (0.25° × 0.25°), in particular the southern part of the Korean peninsula and the Japanese Archipelago. This difference might be caused by poor geographical prescription (e.g. topography, land-use distribution)

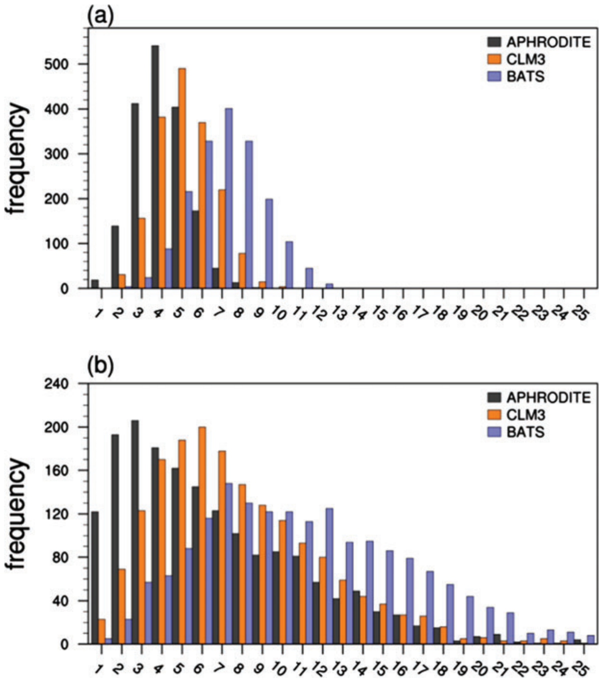

Figure 3. Frequency distribution of daily precipitation averaged over entire domain and South China during the summer season (JJA) derived from APHRODITE, BATS and CLM3 simulations. Here, *x*-axis denotes the intensity of daily precipitation (mm day^{-1}). (a) Entire domain, (b) South China.

in the global reanalysis system with relatively coarse resolution.

Overall, both simulations are in qualitatively good agreement with the observed distribution, capturing some gradient patterns such as more precipitation in the southern China and less precipitation in the northwest China. However, the discrepancy in the quantitative aspect seems to cause the differentiated performance between the two simulations. The biases of the BATS and CLM3 simulations over land areas are 2.5 and 0.8 mm day^{-1}, respectively (Figure1(g) and (h)). The BATS simulation tends to systematically overestimate the precipitation, leading to a strong wet bias across the whole domain. Replacing BATS with the CLM3 land-surface scheme substantially reduces the wet biases that are seen in the BATS simulation. In particular, a dramatic improvement of CLM3 simulation is found in South China. The large difference between the BATS and CLM3 simulations demonstrates the significant sensitivity in the simulation of precipitation to the choice of land-surface scheme. To address the statistical significance of the difference derived from the two simulations, we carry out a two-tailed *t*-test and overlay dots in the areas where the differences between CLM3 and BATS are statistically significant at the 99% confidence level (Figure 1(f)). The dot coverage over the majority of regions reveals that the BATS and CLM3 land-surface schemes lead to a statistically significant difference in mean precipitation.

The 19-year summer simulation makes it possible to assess the performance in capturing the interannual variability. Figure 2 shows the time series of JJA mean precipitation averaged over the entire domain (Lat: 20°N – 50°N and Lon: 108°E – 140°E) and South China (Lat: 20°N – 30°N and Lon: 108°E – 122°E). We present the sub-regional pattern over South China because this area exhibits the largest difference of mean precipitation between the two simulations (Figure 1(f)) and corresponds to localized maximum precipitation (Figure 1(a)–(d)). Figure 2 also includes the anomalies computed by subtracting JJA mean climatology throughout 1989–2007. The presentations of JJA mean time series give insight into the consistency of simulated precipitation pattern across the different years. On the other hand, anomalies with respect to their respective mean climatology demonstrate more clearly the ability to capture observed interannual variability because of the elimination of systematic bias in the underlying mean climate of each simulation.

First, the overestimated error of the BATS simulation is probably not a random feature of specific year, but a rather consistent pattern in different years throughout whole period. The CLM3 simulation also shows some positive bias, but its magnitude is fairly reduced. The BATS simulation produces more precipitation than CLM3, regardless of year and region. In general, the CLM3 simulation is in quantitatively good agreement with observation as compared to the BATS simulation.

Even though both simulations systematically overestimate JJA mean precipitation, the anomalies obtained by subtracting the climatological mean that contains their systematic errors show that both simulations, but particularly the CLM3 simulation, are capable of capturing the observed interannual variability in terms of direction and magnitude. The range of interannual variability in the BATS simulation is more exaggerated over South China compared to the observed one. The correlation coefficients in the temporal evolution of CLM3 and BATS with observation are 0.92 and 0.77 over the entire domain, and 0.92 and 0.88 over South China, respectively. Therefore, the CLM3 simulation shows more skillful performance not only in quantitative aspect but also in its evolutionary feature compared to BATS.

Analysis of the mean precipitation is not sufficiently appropriate to estimate accurate performance of precipitation due to the possibility of hidden errors originating from the frequency and intensity of each precipitation event, irrespective of the reasonable performance of the mean precipitation. Therefore, we examine in more detail the frequency and intensity of daily precipitation. Here, we define a precipitation event as a daily precipitation value greater than or equal to 1.0 mm. The JJA mean intensity of daily precipitation is computed by mean of wet days with precipitation event.

The frequency distribution of daily precipitation again clearly reveals the different behaviour of the BATS and CLM3 simulations. Figure 3 shows the frequency distribution as a function of intensity of daily precipitation averaged over the entire domain and South China, i.e. the same regions as those used for the analysis of Figure 2. Consistent with mean spatial pattern, the distribution of BATS simulation tends to be skewed to right side in both regions,

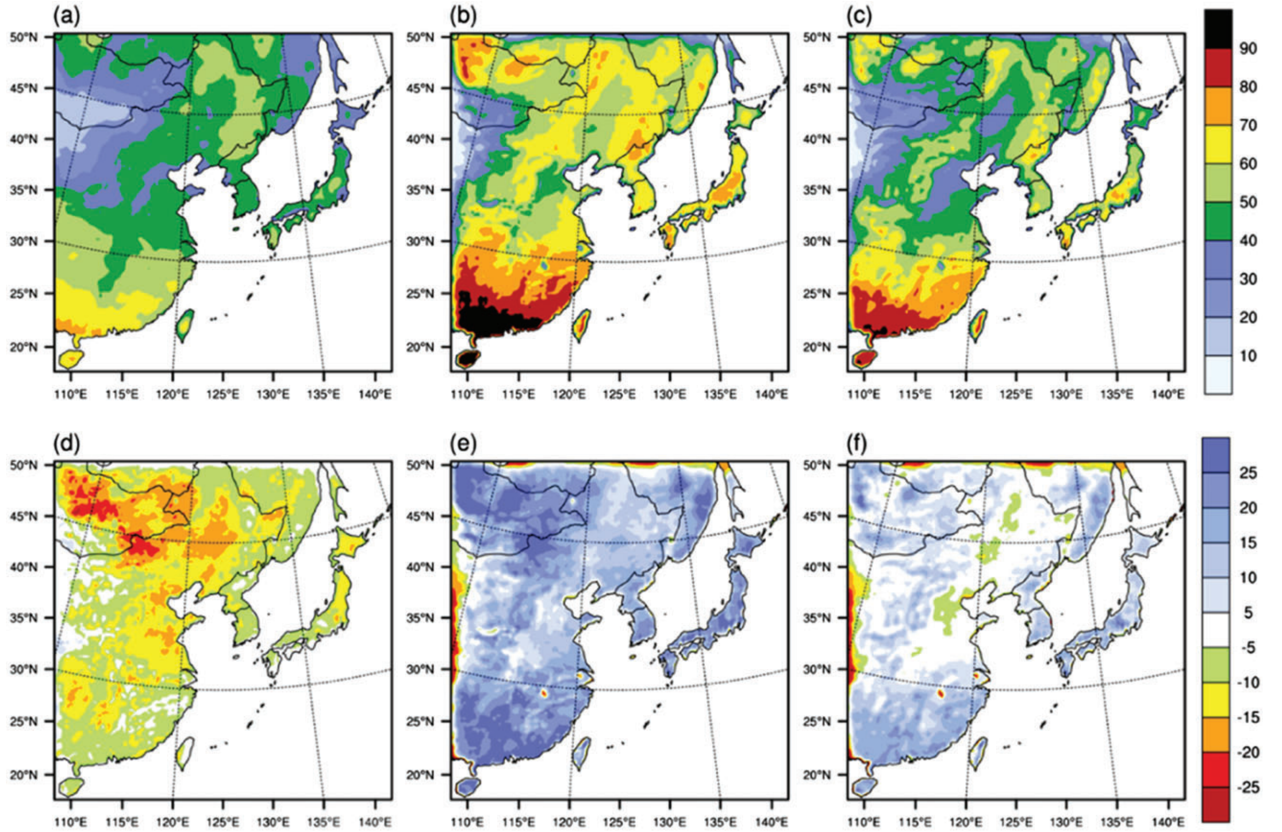

Figure 4. Spatial distribution of frequency of daily precipitation derived from APHRODITE observation, BATS and CLM3 simulations (a–c) and the difference between the two simulations, CLM3−BATS, (d) and the two simulations and APHRODITE, BATS−APHRODITE and CLM3−APHRODITE (e,f) during the summer season (JJA) (%).

being spread out toward longer tails. This behaviour indicates the more frequent occurrence of higher intensity precipitation compared to APHRODITE observation. Daily precipitation from CLM3 simulation is also distributed slightly shifted to the right side against APHRODITE, but its general shape and its relative ratio of the frequency corresponding to each column are much closer to those of APHRODITE.

Moving to the spatial distribution, the CLM3 simulation offers better agreement with observation in both frequency (Figure 4) and intensity (Figure 5), compared to the BATS simulation, which is in line with the mean precipitation. Interestingly, the frequency and intensity exhibit different behaviours. On the basis of the difference between the two simulations (Figures 4(d) and 5(d)), the frequency shows a larger difference in the relatively cold and dry regions (e.g. Mongolia) while the difference of intensity becomes more pronounced in the relatively warm and humid regions (e.g. South China). The northwest area around Mongolia is characterized by less precipitation. However, BATS tends to often produce unrealistic precipitation over that dry region. In fact, Im *et al.* (2014b) reported a similar error in very dry desert regions from the BATS simulation, exposing the deficiency of BATS within the framework of the RegCM modelling system.

To uncover the main factor responsible for the performance difference between the two simulations, we investigate the spatial distribution of convective (Figure 6) and large-scale (Figure 7) precipitation, as well as its ratio (Figure 8). By comparing the convective and large-scale precipitation over land, the portion of convective precipitation in total precipitation (ERA−interim: 59%, BATS: 74%, CLM3: 66%) is larger than that of large-scale precipitation (ERA−interim: 41%, BATS: 26%, CLM3: 34%) in particular for the BATS and CLM3 simulations, indicating that summer precipitation is largely controlled by the convective process of the model over East Asia. An important feature is that the difference between the two simulations is mostly due to convective precipitation rather than large-scale precipitation. The difference of convective precipitation derived from the two simulations shows a pattern that is similar to that of mean precipitation, and is particularly large over South China. Therefore, it is reasonable to assume that the different land-surface schemes significantly influence on the convective activity in the model. Furthermore, the bias of convective precipitation causes the problem embedded in large-scale precipitation due to the very strong connection between the convective and large-scale precipitation schemes in RegCM (Gianotti, 2012). The BATS simulation probably characterizes the suppression of large-scale precipitation from the excessively strong convection over South China. Despite the large overestimation of total precipitation over that region (Figure 1(c)

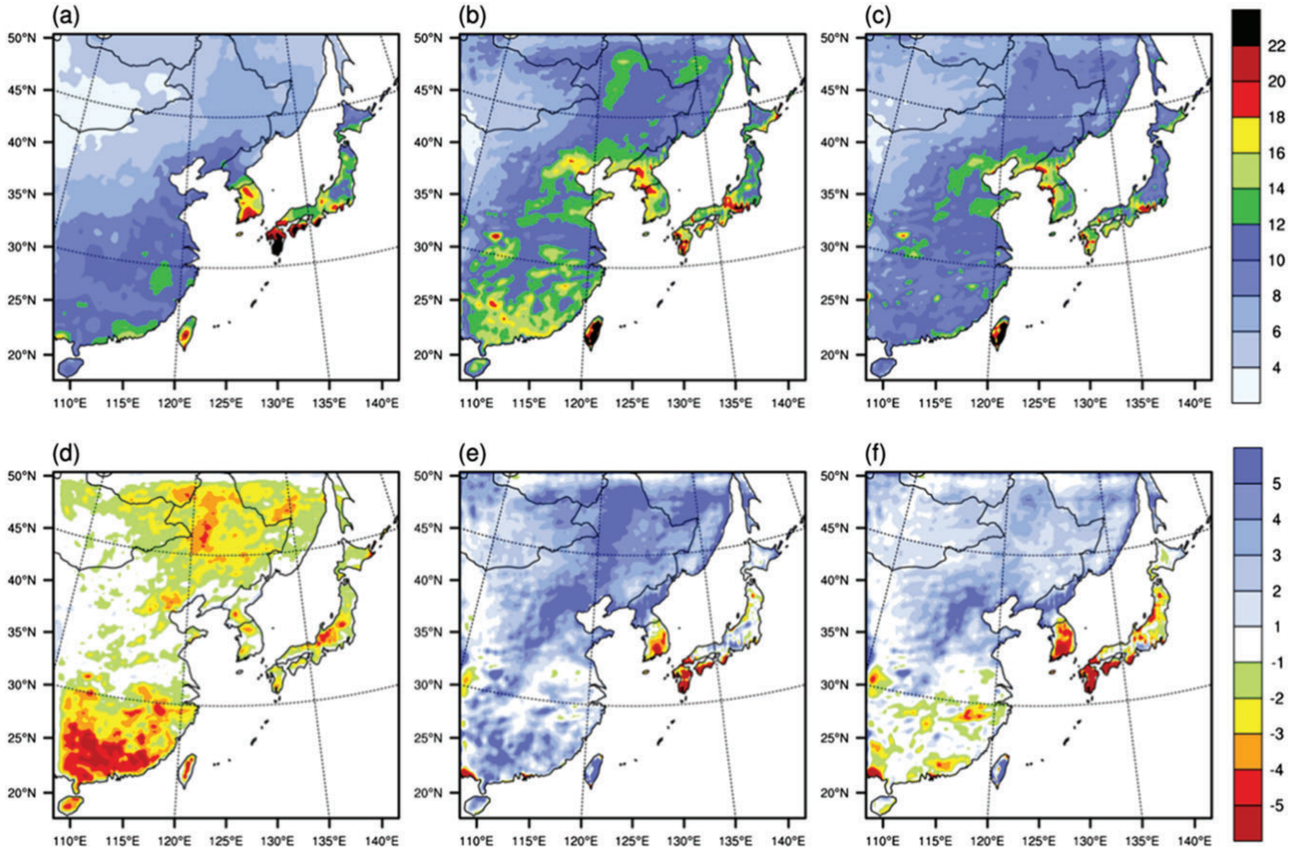

Figure 5. Spatial distribution of intensity of daily precipitation derived from APHRODITE observation, BATS and CLM3 simulations (a–c) and the difference between the two simulations (d) and the two simulations and APHRODITE (e–f) during the summer season (JJA) (mm day^{-1})

and (g)), BATS even underestimates the large-scale precipitation compared to the ERA–interim reanalysis (Figure 7(e)). This implies an improper ratio of convective and large-scale precipitation. In fact, an excessively high ratio over ERA–interim appears across a broad area (Figure 8(b) and (e)). CLM also shows improper ratio in some areas, but the difference between both simulations and ERA–interim reanalysis clearly shows that the coverage and magnitude of errors are reduced in CLM3 than in BATS (Figure 8(e) and (f)). Thus, the ratio of convective and large-scale precipitation further demonstrates the superiority of the CLM3 simulation, which exhibits better agreement with the ERA–interim reanalysis pattern.

Given that both simulations show a significant difference of convective precipitation, we attempt to interpret the physical mechanism that controls the convective activity. As an indicator to represent the process of triggering or the strength of the convection, we compare the CAPE and CIN. Both indices may serve as an important proxy for the convective mass flux (Brockhaus *et al.*, 2008), but with opposite directions. While CIN indicates the negative buoyant energy needed to overcome the free ascent of an air parcel, CAPE is effectively the positive buoyancy of a rising air parcel. Therefore, they can explain the atmospheric instability in an opposite way, accordingly convective initiation. A larger CAPE (CIN) value corresponds to more promotion (suppression) of the triggering of convection. We also present the equivalent potential temperature (θ_e) because a higher θ_e could be an indication of potential instability responsible for a convectively favourable environment, which would increase CAPE (Im *et al.*, 2014a).

Using the vertical dataset with daily time-scale, we calculate θ_e, CAPE and CIN at the most unstable layer over South China. Figure 9 presents the frequency distribution of θ_e, CAPE and CIN derived from the ERA–interim reanalysis and BATS and CLM3 simulations.

In general, the behaviours differ in both simulations for all three indices. Hence, the comparison of these three indices demonstrates that different land-surface schemes can significantly modulate the atmospheric thermodynamic structure, and hence enhance or suppress the triggering of convection. The CLM3 simulation shows considerable improvement in both the general shape of distribution and the relative ratio of each column for all the indices. For example, the BATS simulation produces the second maximum frequency of θ_e between 360 and 365 K, whereas the CLM3 simulation and ERA–interim reanalysis show a sharp drop in that range, so that the BATS distribution is more skewed to the right side than is the ERA–interim reanalysis. The same problem appears in the distribution of CAPE. More specifically, the CAPE derived from the BATS simulation is significantly larger than the corresponding values in the CLM3 simulation. The complete shift of the distribution suggests that it is not a random

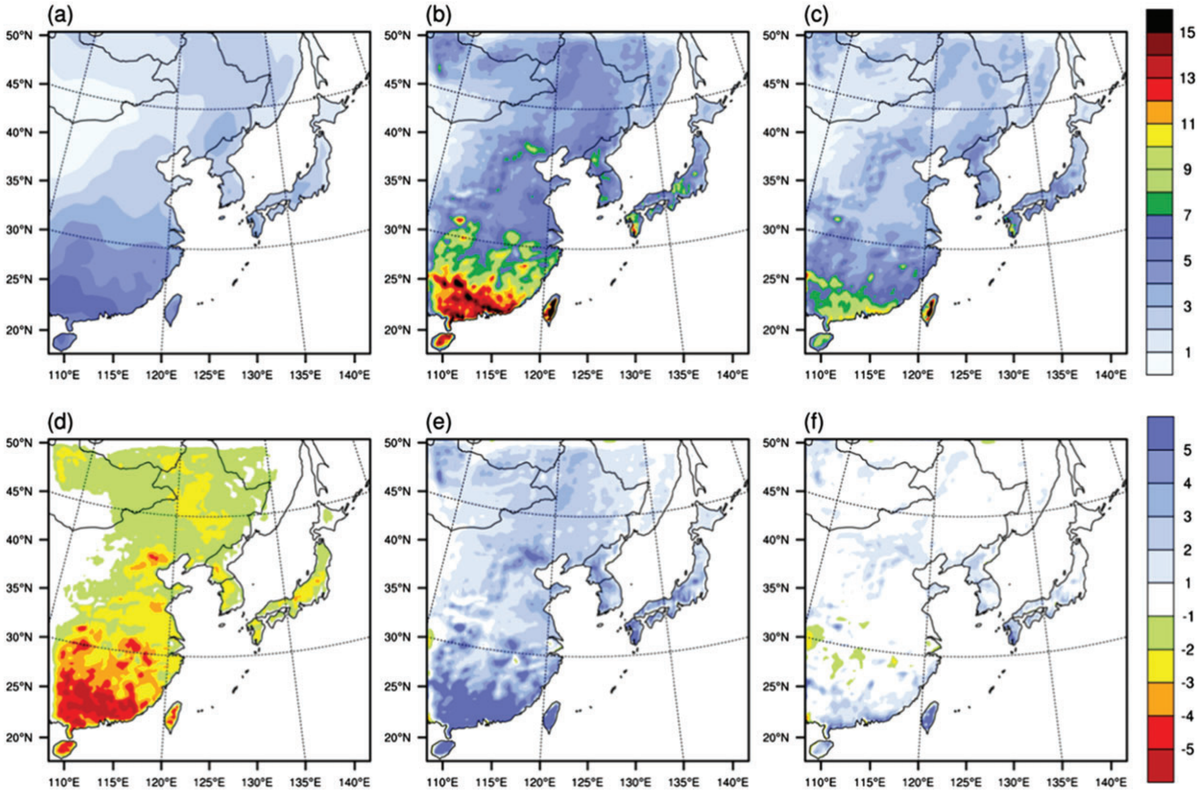

Figure 6. Spatial distribution of convective precipitation derived from the ERA–interim reanalysis, BATS and CLM3 simulations (a–c) and the difference between the two simulations (d) and the two simulations and ERA–interim reanalysis (e–f) during the summer season (JJA) (mm day^{-1}).

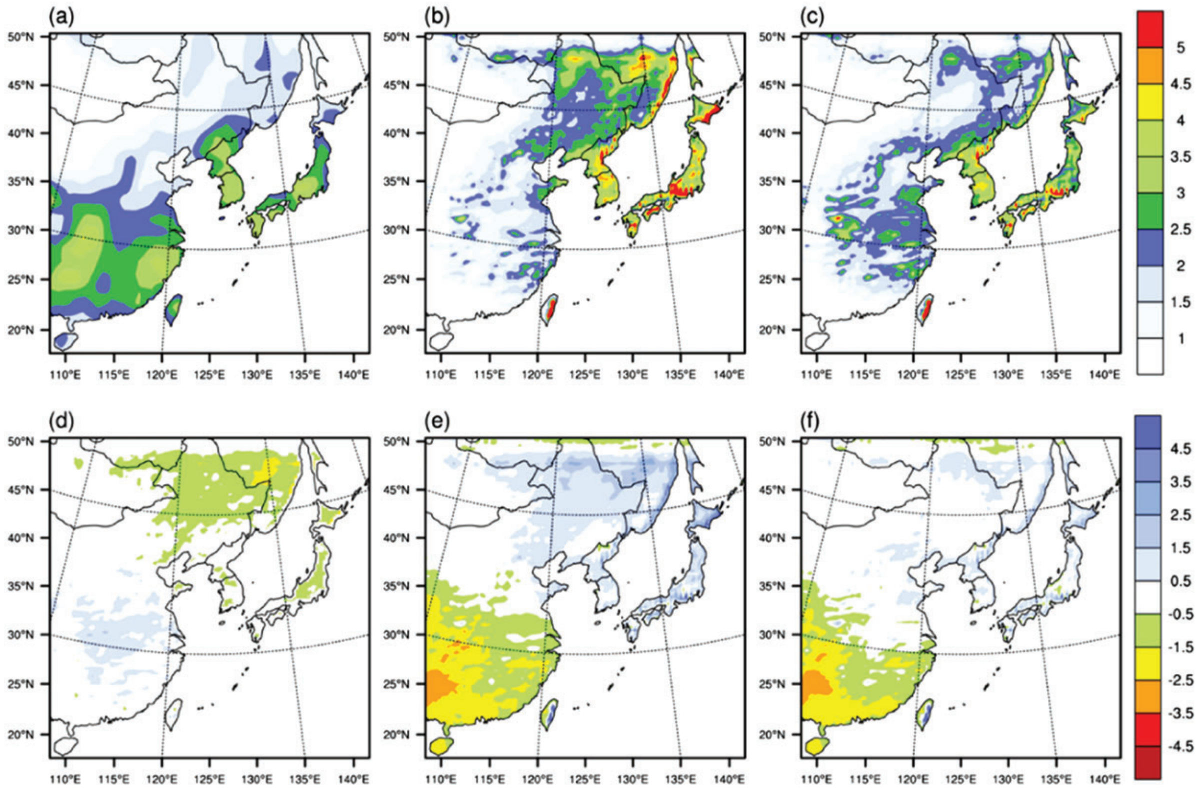

Figure 7. Spatial distribution of large-scale precipitation derived from the ERA–interim reanalysis, BATS and CLM3 simulations (a–c) and the difference between the two simulations (d) and the two simulations and ERA–interim reanalysis (e–f) during the summer season (JJA) (mm day^{-1}).

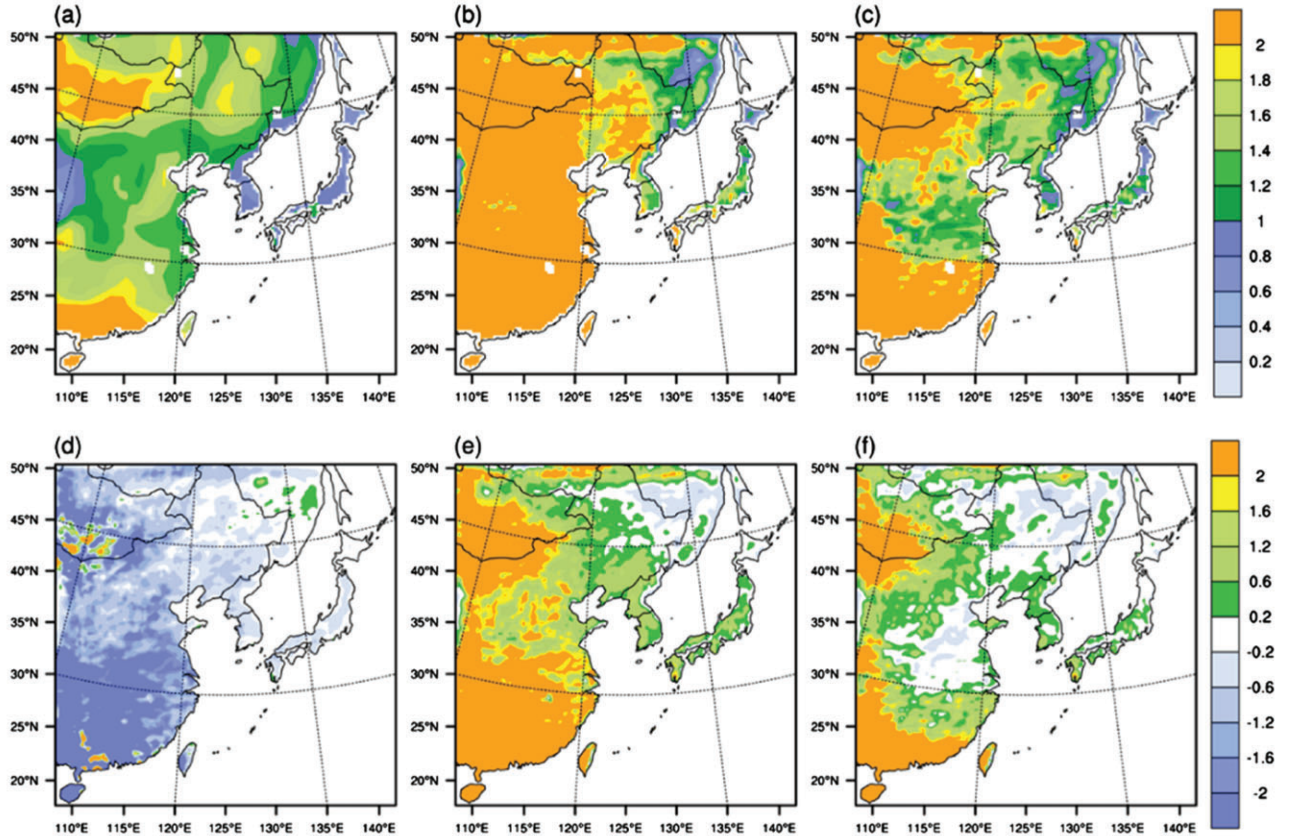

Figure 8. Spatial distribution of ratio of convective and large-scale precipitation derived from the ERA–interim reanalysis, BATS and CLM3 simulations (a–c) and the difference between the two simulations (d) and the two simulations and ERA–interim reanalysis (e–f) during the summer season (JJA) (mm day^{-1}).

feature due to several precipitation events, but rather a consistent pattern characterizing the BATS simulation.

The basic characteristics of the CIN distribution, such as the peak position and relative ratio of each column, are quite different from those of the CAPE distribution. This is natural because CAPE and CIN are opposite measurements of the atmospheric condition to describe the growth and suppression of the triggering of convection. Contrary to θ_e and CAPE, the deficiency of the BATS simulation is exposed in the CIN distribution due to the left-side shift of the maximum frequency. Therefore, the relatively larger CAPE and smaller CIN imply a BATS deficiency in both the intensity and the frequency of convective precipitation, which supports the assumption that deep convection intensity is modulated by CAPE while the occurrence frequency is more controlled by CIN (Mapes, 2000; Myoung and Nielsen-Gammon, 2010).

The processes regulating this divergence of behaviour between CLM3 and BATS simulations are complex and it is very difficult to separately measure the impacts of the land-surface scheme because multiple processes are complicatedly interrelated. Nevertheless, a possible mechanism can be postulated by the soil moisture influence on convective precipitation. The relevant difference of both land-surface schemes is the soil moisture. Figure 10 presents the daily time-series of 19-year climatological soil moisture averaged over South China, which is the same region as that used in calculating the stability indices. In line with previous studies addressing the wet bias of soil moisture (Steiner *et al.*, 2009; Diro *et al.*, 2012), our BATS simulation also produces an excessively wet soil condition compared to that of CLM3. The wetter soil moisture is expected to lead to the higher moist static energy due to the increase of the total flux of heat from the land surface (Im *et al.*, 2014a). Therefore, the BATS simulation produces a more dominant distribution with larger CAPE and smaller CIN. The different behaviour of soil moisture is more a reflection of prescribed input data for surface properties such as soil colour and soil texture, rather than an intrinsic feature of the model itself. Different land surface models use different methods to quantify the impact of vegetation and soil moisture. In this regard, the strongly overestimated soil moisture of BATS over the selected region is largely caused by the uncertainty of soil properties prescribed by the BATS land-surface scheme.

The different features of soil moisture can modulate the relative partitioning of latent and sensible heat fluxes. Figures 11 and 12 present the spatial distribution of the latent and sensible heat fluxes derived from the EAR–interim reanalysis, BATS and CLM3 simulations, and the differences between the two simulations as well as between the two simulations and ERA–interim reanalysis during the summer season. In general, these heat fluxes show opposing spatial patterns, due to differences in the

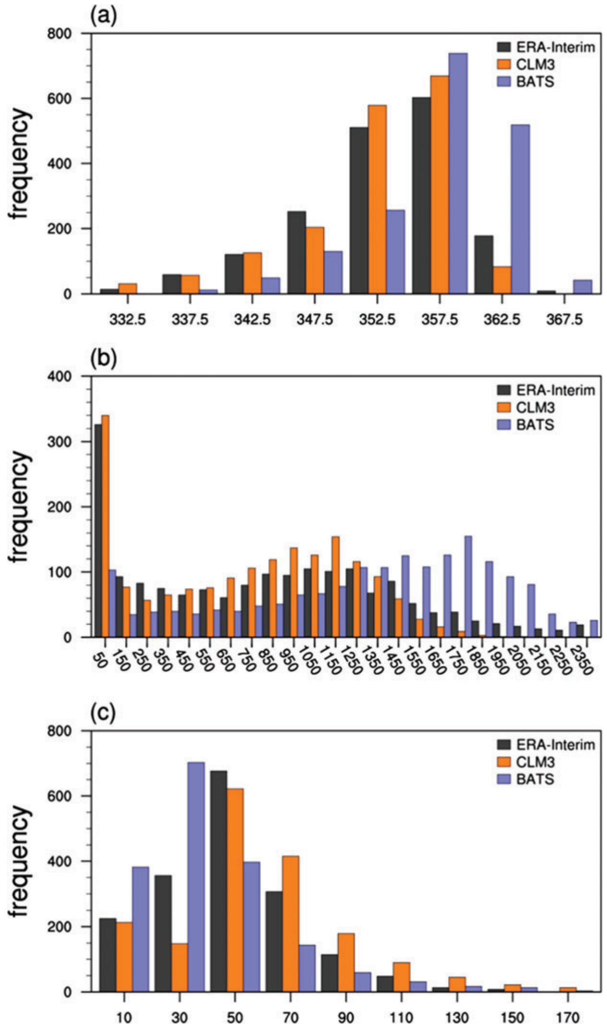

Figure 9. Frequency distribution of equivalent potential temperature (K) (a), CAPE ($J\,kg^{-1}$) (b) and CIN ($J\,kg^{-1}$) (c) derived from the ERA–interim reanalysis, BATS and CLM3 simulations over South China.

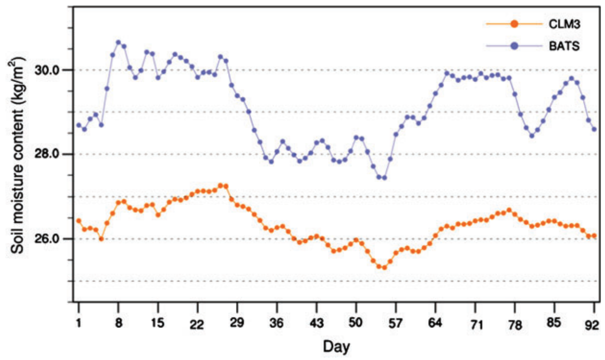

Figure 10. Area-averaged daily time-series of soil moisture simulated by BATS and CLM3 over South China ($kg\,m^{-2}$).

way that heat is transferred over wet and dry regions. Relatively wet (dry) regions are dominated by surface heat release through latent (sensible) heat flux. Figure 11 reveals that errors in simulated latent heat flux tend to correspond with the bias in simulated precipitation. The BATS simulation overestimates the latent heat flux due to the stronger evapotranspiration induced by excessive wet soil moisture. Wetter soil induces not only overestimation of latent heat flux but also underestimation of sensible heat flux because strong cooling simultaneously occurs with moistening of the lower atmosphere. Such errors in both latent and sensible heat fluxes are well revealed in the BATS simulation of the southern China region. This means that soil moisture affects the surface energy budget by modulating the relative partitioning of latent and sensible heat fluxes. Overall, CLM3 demonstrates better performance in terms of adequate spatial distribution and proper magnitude of the latent and sensible heat fluxes. As in our study, Steiner *et al.* (2005, 2009) and Im *et al.* (2014b) demonstrated that the land-surface scheme can improve the simulated surface heat fluxes, emphasizing the important role of land–atmosphere interaction in shaping the climate condition from regional model experiments.

4. Summary and discussion

In this study, we examine the performance of the RegCM4 in simulating the summer precipitation over East Asia. To investigate the impact of the land-surface scheme on the characteristics of daily precipitation, two reproduction experiments incorporating BATS and CLM3 land-surface schemes are performed using the ERA–interim reanalysis as the initial and boundary condition. All model configurations are the same except for the land-surface scheme.

Although many sensitivity studies of physical parameterizations have been conducted to improve the regional climate simulation over East Asia, most of them have focussed on the superiority of one parameterization over another based on the validation of mean climatology (e.g. Steiner *et al.*, 2005; Chen *et al.*, 2012; Bao, 2013). In this study, in addition to analysis of seasonal mean climatology and interannual variability, we emphasize the impact of land-surface schemes on convective process for determining the characteristics of daily precipitation and the physical mechanism that explains the different performance caused by the BATS and CLM3 land-surface schemes. Despite applying the same Emanuel convection scheme, the different land-surface schemes produce different performances in daily precipitation, primary due to the different skill in capturing the characteristics of convective precipitation. A large sensitivity of precipitation to different land-surface schemes is comparable to the results induced by cumulus parameterization (Singh *et al.*, 2006; Im *et al.*, 2008), which highlights the important role played by land–atmosphere interactions in determining the performance of precipitation within the RegCM4 modelling system. Since the land-surface process strongly depends on the convection schemes, we also carried out 1-year (1989) sensitivity experiments implementing BATS and CLM3 land-surface schemes in combination with the Grell scheme with Fritch-Chappell closure (Figure S3). Even

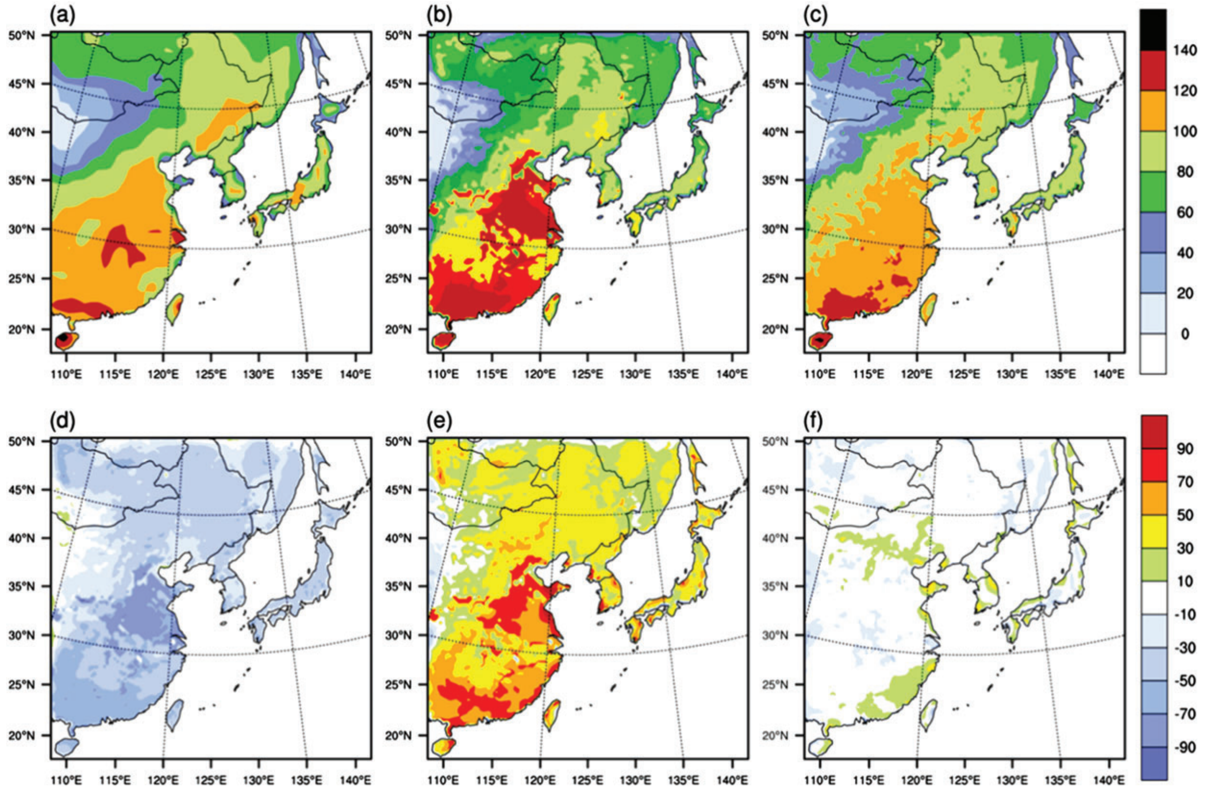

Figure 11. Spatial distribution of latent heat fluxes derived from the ERA–interim reanalysis, BATS and CLM3 simulations (a–c) and the difference between the two simulations (d) and the two simulations and ERA–interim reanalysis (e–f) during the summer seas (JJA) (W m^{-2}).

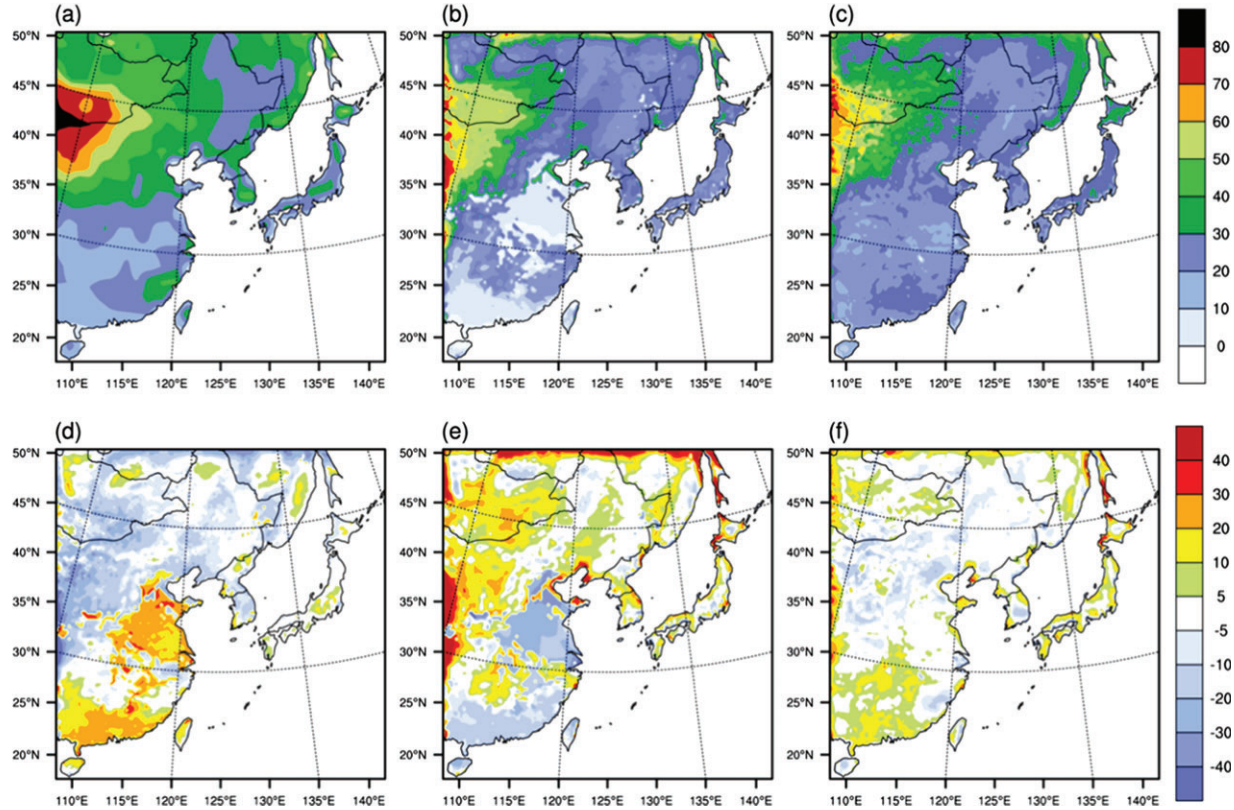

Figure 12. Spatial distribution of sensible heat fluxes derived from the ERA–interim reanalysis, BATS and CLM3 simulations (a–c) and the difference between the two simulations (d) and the two simulations and ERA–interim reanalysis (e,f) during the summer seas (JJA) (W m^{-2}).

though such a single-year simulation is insufficient to represent the typical pattern of summer climatology, the BATS and CLM3 simulations with the Grell scheme are similar to the simulations attained from 19-year mean climatology as seen in this study. Therefore, the BATS simulation tends to consistently overestimate the mean precipitation over East Asia, irrespective of the convection scheme within the RegCM modelling system.

Overall, the CLM3 simulation offers better agreement of mean, frequency and intensity of daily precipitation with the observed estimates, and presents a substantial reduction in the wet bias seen in the BATS simulation. In fact, the wet bias of the BATS simulation is a well-documented deficiency across various study regions (e.g. East Asia for Steiner *et al.*, 2005; West Africa for Steiner *et al.*, 2009 and Im *et al.*, 2014b; Central America and Mexico for Diro *et al.*, 2012). The improvement in the characteristics of daily precipitation of the CLM3 simulation can be attributed to the improved thermodynamic structure (as described by the stability indices) and the resultant convective precipitation. The CLM3 simulation exhibits a more reasonable performance with respect to the frequency distribution of the θ_e, CAPE and CIN indices. The better results of the CLM3 simulation can be further ascribed to the simultaneous interpretation with soil moisture. In fact, earlier studies have demonstrated that soil moisture strongly affects convective instability and the resultant convective precipitation (Alfieri *et al.*, 2008; Myoung and Nielsen-Gammon, 2010; Hauck *et al.*, 2011). Higher values of soil moisture lead to enhanced latent heat flux, which is supposed to be responsible for more intense convective rainfall. The BATS simulation tends to inadequately partition surface heat fluxes due to wet soil moisture, and the strongly enhanced evaporation releases excessive energy to the atmosphere, leading to an unrealistically unstable condition.

The results presented in this study support the assertion that parameterizations of the land surface are critical for improving model performance. Based on our analysis, we suggest that the RegCM4 simulation with CLM3 land-surface scheme is capable of reproducing the major characteristics of summer climate over East Asia, such as daily precipitation, surface heat flux and atmospheric thermodynamic structure. This study will enhance the reliability of the RegCM4 modelling system with the CLM3 land-surface scheme for future climate projection over this region.

Acknowledgements

This work was carried out with the support of Korea Meteorological Administration Research and Development Program under Grant CATER 2012-3083 and Rural Development Administration Cooperative Research Program for Agriculture Science and Technology Development under Grant Project No. PJ009353, Republic of Korea.

Supporting Information

The following supporting information is available as part of the online article:

Figure S1: Spatial distribution of JJA mean precipitation derived from APHRODITE, the simulations of CLM3 land surface and Emanuel convection scheme with 7-day (staring date: 25 May, indicated as 0525 in figure) and 1-month (staring date: 1 May, indicated as 0501 in figure) spin-up period, and the difference between the two simulations and the two simulations and APRODIETE.

Figure S2: Spatial distribution of JJA mean precipitation derived from APHRODITE, the simulations of BATS land surface and Emanuel convection scheme with 7-day (staring date: 25 May, indicated as 0525 in figure) and 1-month (staring date: 1 May, indicated as 0501 in figure) spin-up period, and the difference between the two simulations and the two simulations and APRODIETE.

Figure S3: Spatial distribution of JJA mean precipitation (1989) derived from APHRODITE observation, and BATS and CLM3 simulations in combination with Emanuel and Grell convection schemes.

References

Alfieri L, Claps P, D'Odorico P, Laio F, Over TM. 2008. An analysis of the soil moisture feedback on convective and stratiform precipitation. *J. Hydrometeorol.* **9**: 280–291.

Anthes RA, Kuo YH, Hsie EY, Low S, Bettge TW. 1989. Estimation of skill and uncertainty in regional numerical models. *Q. J. R. Meteorol. Soc.* **115**: 763–806.

Bao Y. 2013. Simulations of summer monsoon climate over East Asia with a regional climate model (RegCM) using Tiedtke convective parameterization scheme (CPS). *Atmos. Res.* **134**: 35–44.

Brockhaus P, Luthi D, Schar C. 2008. Aspects of the diurnal cycle in a regional climate model. *Meteorol. Z.* **17**: 433–443.

Cha D-H, Lee D-K, Hong S-Y. 2008. Impact of boundary layer processes on seasonal simulation of the East Asian summer monsoon using a Regional Climate Model. *Meteorol. Atmos. Phys.* **100**: 53–72.

Chen L, Ma Z, Fan X. 2012. A comparative study of two land surface schemes in WRF model over Eastern China. *J. Trop. Meteorol.* **18**: 445–456.

Dee DP, Uppala SM, Simmons AJ, Berrisford P, Poli P, Kobayashi S, Andrae U, Balmaseda MA, Balsamo G, Bauer P, Bechtold P, Beljaars ACM, van de Berg L, Bidlot J, Bormann N, Delsol C, Dragani R, Fuentes M, Geer AJ, Haimberger L, Healy SB, Hersbach H, Hólm EV, Isaksen L, Kållberg P, Köhler M, Matricardi M, McNally AP, Monge-Sanz BM, Morcrette JJ, Park BK, Peubey C, de Rosnay P, Tavolato C, Thépaut JN, Vitart F. 2011. The ERA-interim reanalysis: configuration and performance of the data assimilation system. *Q. J. R. Meteorol. Soc.* **137**: 553–597.

Diro GT, Rauscher SA, Giorgi F, Tompkins AM. 2012. RegCM4: sensitivity of seasonal climate and diurnal precipitation over Central America to land and sea surface schemes in RegCM4. *Clim. Res.* **52**: 31–48.

Emanuel KA, Rothman MZ. 1999. Development and evaluation of a convection scheme for use in climate models. *J. Atmos. Sci.* **56**: 1756–1782.

Fu CB, Wang SY, Xiong Z, Gutowski WJ, Lee DK, McGregor J, Sato Y, Kato H, Kim JW, Su MS. 2005. Regional climate model Intercomparison Project for Asia. *Bull. Am. Meteorol. Soc.* **86**: 257–266.

Gao X, Shi Y, Song R. 2008. Reduction of future monsoon precipitation over China: comparison between a high resolution RCM simulation and the driving GCM. *Meteorol. Atmos. Phys.* **100**: 73–86, DOI: 10.1007/s00703-008-0296-5.

Gianotti RL. 2012. Regional Climate Modeling over the Maritime Continent: Convective Cloud and Rainfall Processes. Ph.D. dissertation, Massachusetts Institute of Technology, 306.

Giorgi F, Coppola E, Solmon F, Mariotti L, Sylla MB, Bi X, Elguindi N, Diro GT, Nair V, Giuliani G, Cozzini S, Güttler I, O'Brien TA,

Tawfik AB, Shalaby A, Zakey AS, Steiner AL, Stordal F, Sloan LC, Brankovic C. 2012. RegCM4: model description and preliminary test over multi CORDEX domains. *Clim. Res.* **52**: 7–29.
Grell GA, Dudhia J, Stauffer DR. 1994. *A description of the fifth generation Penn State/NCAR mesoscale model (MM5)*. NCAR Technical Note NCAR/TN-398+STR, NCAR, Boulder, CO.
Hauck C, Barthlott C, Krauss L, Kalthoff N. 2011. Soil moisture variability and its influence on convective precipitation over complex terrain. *Q. J. R. Meteorol. Soc* **137**: 42–56.
Holtslag AAM, de bruijn EIF, Pan H-L. 1990. A high resolution air mass transformation model for short-range weather forecasting. *Mon. Weather Rev.* **118**: 1561–1575.
Hong S-Y, Choi J. 2006. Sensitivity of the simulated regional climate circulations over East Asia in 1997 and 1998 summers to three convective parameterization schemes. *J. Korean Meteorol. Soc.* **42**: 361–378.
Huang W-R, Chan JCL, Au-Yeung AYM. 2012. Regional climate simulation of summer diurnal rainfall variations over East Asia and Southeast China. *Clim. Dyn.* **40**: 1625–1642, DOI: 10.1007/s00382-012-1457-2.
Im ES, Ahn JB, Remedio AR, Kwon WT. 2008. Sensitivity of the regional climate of East/Southeast Asia to convective parameterizations in the RegCM3 modeling system. Part 1: focus on the Korean peninsula. *Int. J. Climatol.* **28**: 1861–1877.
Im E-S, Marcella MP, Eltahir EAB. 2014a. Impact of potential large-scale irrigation on the West African Monsoon and its dependence on location of irrigated area. *J. Clim.* **27**: 994–1009.
Im E-S, Gianotti RL, Eltahir EAB. 2014b. Improving the simulation of the West African Monsoon using the MIT Regional Climate Model. *J. Clim.* **27**: 2209–2229.
Kang H-S, Hong S-Y. 2008. Sensitivity of the simulated East Asian summer monsoon climatology to four convective parameterization Schemes. *J. Geophys. Res.* **113**: D15119, DOI: 10.1029/2007 JD00969.
Kang H-S, Cha D-H, Lee D-K. 2005. Evaluation of the mesoscale model/land surface model (MM5/LSM) coupled model for East Asian summer monsoon simulations. *J. Geophys. Res.* **110**: D10105, DOI: 10.1029/2004JD005266.
Kiehl JT, Hack JJ, Bonan GB, Boville BA, Briegleb BP, Williamson DL, Rasch PJ. 1996. *Description of NCAR Community Climate Model (CCM3)*. NCAR Technical Note NCAR/TN-420+STP, NCAR, Boulder, CO.
Mapes BE. 2000. Convective inhibition, subgrid-scale triggering energy, and stratiform instability in a toy tropical wave model. *J. Atmos. Sci.* **57**: 1515–1535.
Min H-J, Jhun J-G. 2010. The changes in the East Asian summer monsoon simulated by the MIROC3.2 high resolution coupled model under global warming scenarios. *Asia Pac. J. Atmos. Sci* **46**: 73–88.
Myoung B, Nielsen-Gammon JW. 2010. The convective instability pathway to warm season drought in Texas. Part I: the role of convective inhibition and its modulation by soil moisture. *J. Clim.* **23**: 4461–4473.
Oh SG, Suh MS, Myoung JM, Cha DH. 2011. Impact of boundary conditions and cumulus parameterization schemes on regional climate simulation over South-Korea in the CORDEX - East Asia domain using the RegCM4 model. *J. Korean Earth Sci.* **32**(4): 373–387.
Pal JS, Small EE, Eltahir EAB. 2000. Simulation of regional-scale water and energy budgets: representation of subgrid cloud and precipitation processes within RegCM. *J. Geophys. Res.* **105**: 29579–29594.
Park JH, Oh SG, Suh MS. 2013. Impact of boundary conditions on the precipitation simulation of RegCM4 in the CORDEX East Asia domain. *J. Geophys. Res.* **118**: 1652–1667, DOI: 10.1002/jgrd.5015.
Singh GP, Oh JH, Kim JY, Kim OY. 2006. Sensitivity of summer monsoon precipitation over East Asia to convective parameterization scheme in RegCM3. *SOLA* **2**: 29–32, DOI: 10.2151/sola.2006-008.
Steiner AL, Pal JS, Giorgi F, Dickinson RE, Chameides WL. 2005. The coupling of the Common Land Model (CLM0) to a regional climate model (RegCM). *Theor. Appl. Climatol.* **82**: 225–243.
Steiner AL, Pal JS, Rauscher SA, Bell JL, Diffenbaugh SN, Boone A, Sloan LC, Giorgi F. 2009. Land surface coupling in regional climate simulations of the West African monsoon. *Clim. Dyn.* **33**: 869–892, DOI: 10.1007/s00382-009-0543-6.
Yatagai A, Arakawa O, Kamiguchi K, Kawamoto H, Nodzu MI, Hamada A. 2009. A 44-year daily gridded precipitation dataset for Asia based on a dense network of rain gauges. *SOLA* **5**: 137–140, DOI: 10.2151/sola.2009-035.
Yhang YB, Hong S-Y. 2008. Improved physical processes in a regional climate model and their impact on the simulated summer monsoon circulations over East Asia. *J. Clim.* **21**: 963–979.